Electronic supplementary materials *Mendeleev Commun.*, 2023, **33**, 61–63

Chain photosolvation of *trans,trans,trans*-[$Pt^{IV}(py)_2(N_3)_2(OH)_2$] complex prospective as a light-activated antitumor agent

Grigory I. Zhdankin, Vjacheslav P. Grivin, Victor F. Plyusnin, Pavel A. Tkachenko, Danila B. Vasilchenko and Evgeni M. Glebov

S1. Experimental details.

Elemental CHN analysis was carried out on a CHNS analyser Vario MICRO cube.

NMR spectra (at 24°C) were recorded at 500.13 (^1H), 125.76 (^{13}C), 36.14 (^{14}N) and 107.5 MHz (^{195}Pt) using an Avance III 500 Bruker spectrometer with a 5 mm broad-band probe. δ (ppm) values are reported relative to the external or internal reference, which were TMS (^1H), $CDCl_3$ (^{13}C), 1M aqueous solution of $NaNO_3$ (^{14}N) and 2 M solution of $H_2[PtCl_6]$ in 1 M hydrochloric acid (^{195}Pt).

UV absorption spectra were recorded using Agilent 8453 (Agilent Technologies) and Varian Cary 50 (Varian Inc.) spectrophotometers.

Stationary photolysis (308 nm) was performed by radiation of a XeCl excilamp (half width of light pulse, 5 nm; pulse duration, 1 μs; frequency, 200 kHz; incident light flux, 8×10^{15} photons·cm^{-2} s^{-1}) [S1]. Quantum yields were calculated using a ferrioxalate actinometer [S2] to measure light quanta flux. All the quantum yields measurements were repeated three times.

The laser flash photolysis experiments were performed using excitation by 4th harmonics of a Nd:YAG laser (Lotis TII, Belarus, 266 nm, 5 ns pulse duration, up to 10 mJ/pulse energy). The setup was described in detail in works [S3, S4]. Laser pulse energy was measured by means of light power meter SOLO 2 (Gentec, Canada).

S2. Synthesis and characterization of Complex 1

Complex **1** (Scheme S1) was synthesized as described in work [S5] and characterized by means of elemental analysis, NMR and UV-spectroscopy.

Elemental analysis. Anal. Calcd (Found) for $C_{10}H_{12}N_8O_2Pt$: C, 25.48 (25.3); H, 2.57 (2.5); N, 23.77 (23.4).

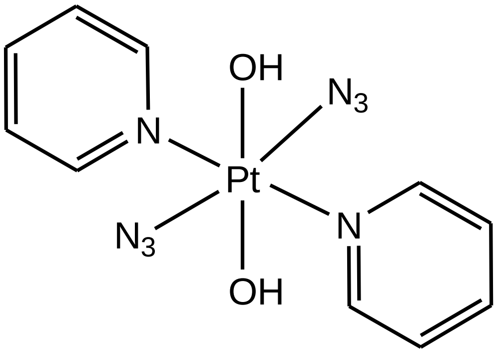

Scheme S1. *Trans,trans,trans*-[Pt^{IV}(N$_3$)$_2$(py)$_2$(OH)$_2$] (Complex **1**).

NMR. δ (ppm) values are reported relative to the external or internal reference, which were TMS (^{1}H), CDCl$_3$ (^{13}C), 1M aqueous solution of NaNO$_3$ (^{14}N) and 2 M solution of H$_2$[PtCl$_6$] in 1 M hydrochloric acid (^{195}Pt). The spectra are shown in Fig. S1.

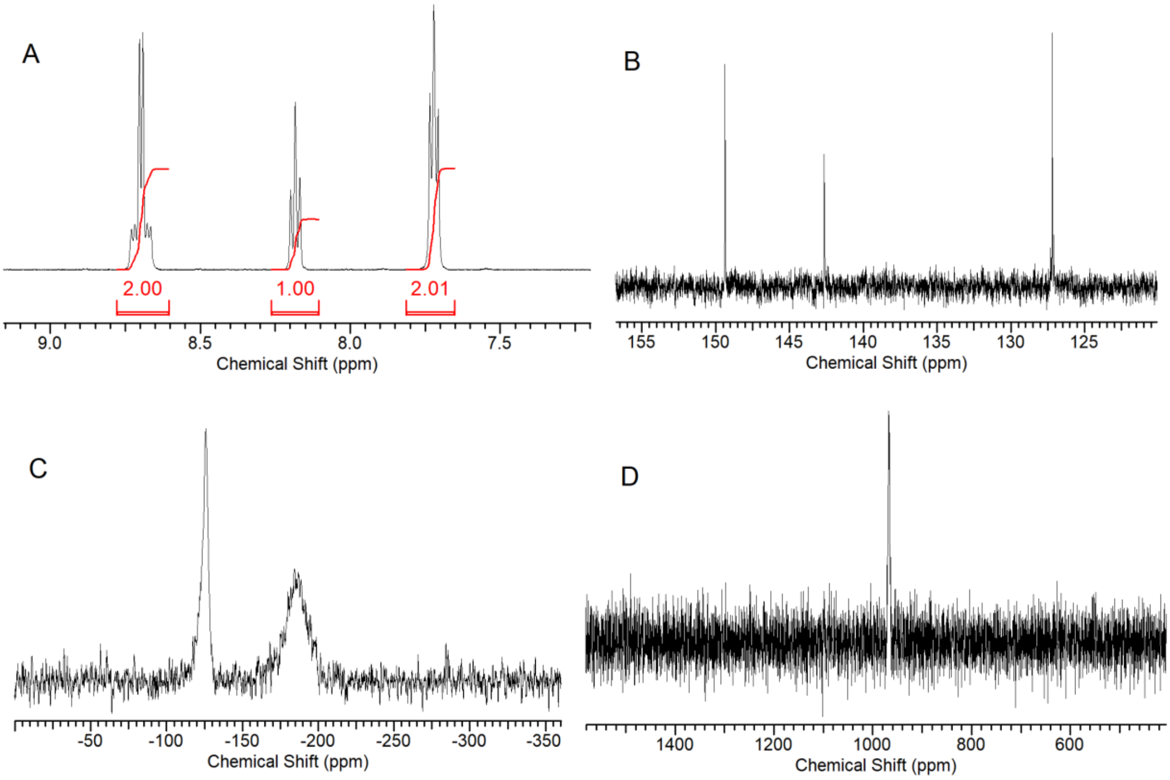

Figure S1. ^{1}H (A), ^{13}C (B), ^{14}N (C) and ^{195}Pt (D) NMR spectra of the aqueous solution of **1**.

UV spectroscopy. UV spectrum of Complex 1 in aqueous solution is shown in Fig. S2.

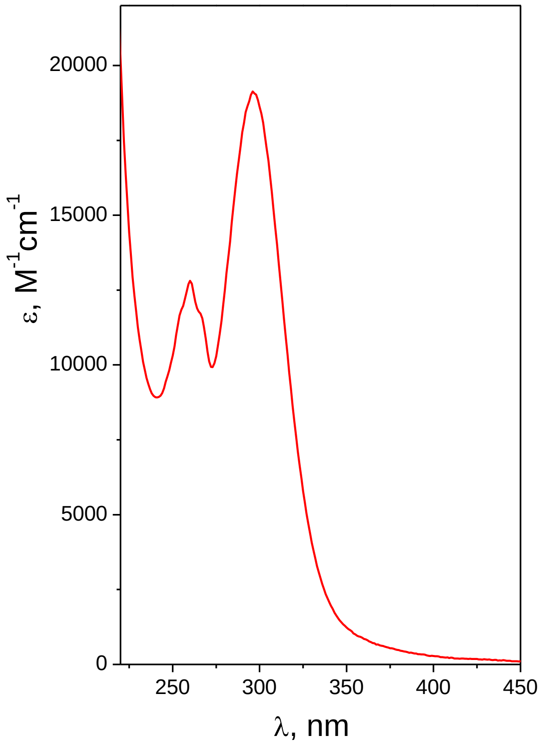

Figure S2. UV spectrum of Complex 1.

S3. Photoaquation of complex 1. Quantum yields determination.

Photoaquation. Quantum yield of photoaquation was determined at the first stage of photolysis when the isosbestic point at 272 nm is conserved. Formula (S1) was used for calculations.

$$\varphi = \frac{\dfrac{dD^{\lambda}}{dt}}{\Delta\varepsilon^{\lambda} L \left(\dfrac{I_0}{V}\right)\left(1-10^{-D^{ex}}\right)} \qquad \text{(S1)}$$

where $\frac{dD^{\lambda}}{dt}$ is the time derivative of absorption at the selected wavelength (in our case absorption maximum at 296 nm was used) determined at the initial part of the photokinetic curve; $\Delta\varepsilon^{\lambda}$ (M^{-1}cm^{-1}) is the difference in molar absorption coefficients of initial compound and photoproduct at the registration wavelength; I_0 is the intensity of incident light flux (moles of quanta per second), V (cm^3) is the sample volume, L (cm) is the optical pathway, D^{ex} – is the sample absorption at the excitation wavelength (308 nm in our case).

The spectral changes in the course of Complex **1** irradiation are shown in Fig. S3. The value of $\frac{dD^{\lambda}}{dt}$ was determined from the initial parts of the photokinetic curves. Incident light intensity I_0 was measured using modified ferrioxalate actinometer [S2]. The value of $\Delta\varepsilon^{\lambda}$ was estimates as follows. The value of molar absorption coefficient of **1** at 296 nm is 19130 $M^{-1}cm^{-1}$. Irradiation was performed till the moment when isosbestic point at 272 nm still existed (curve 12 in Fig. S3). Further irradiation resulted in gradual decrease of absorption at all wavelengths, and the rate of this decrease was much smaller that that of the first process. Therefore, we considered curve 12 as the spectrum of the aquated complex $[Pt^{IV}(Py)_2(N_3)(OH)_2(H_2O/OH)]^{+/0}$. In this case, its molar absorption coefficient at 296 nm is 10540 $M^{-1}cm^{-1}$. It gave the value of $\Delta\varepsilon^{296nm}$ equal to 8770 $M^{-1}cm^{-1}$ which was further used for quantum yield determination. For the conditions of the experiment illustrated by Fig. S3 the value of the photoaquation quantum yield was 0.13.

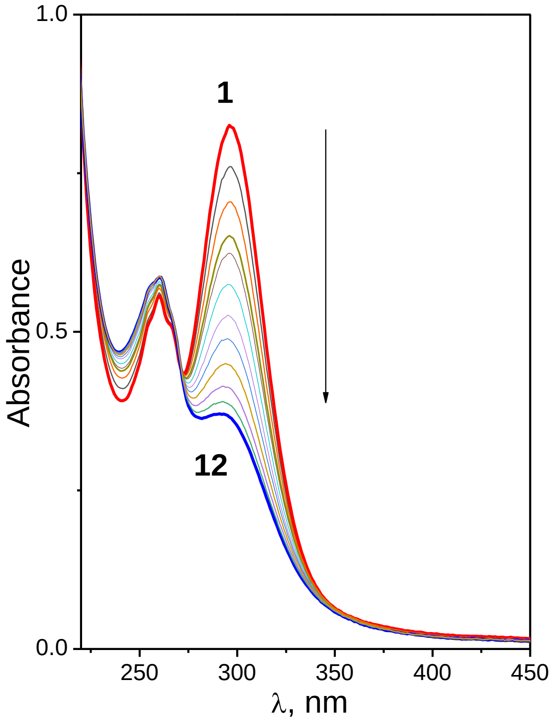

Figure S3. Changes in the UV spectrum of complex **1** (4.3×10^{-5} M, 1 cm cell, air-saturated aqueous solution) in the course of stationary photolysis (308 nm). Curves 1 and 12 correspond to 0 and 232 c of irradiation. Curve 12 was considered as the spectrum of the aquated complex *trans*-$[Pt^{IV}(Py)_2(N_3)(OH)_2(H_2O)]^+$ or *trans*-$[Pt^{IV}(Py)_2(N_3)(OH)_3]$.

Photoreduction. Quantum yield of photoreduction was estimated at the second stage of photolysis when the gradual decrease of absorption in the whole spectral range was observed (Fig. S4). Quantum yield was calculated by formula (1) with the value of $\Delta\varepsilon^{296nm}$ equal to difference between absorptions of *trans*-$[Pt^{IV}(Py)_2(N_3)(OH)_2(OH/H_2O)]^{0/+}$ and Pt(II) complexes. The structure of Pt(II) products was not determined in this work. According to work [S6] the final product is *trans*-$[Pt^{II}(Py)_2(OH/H_2O)_2]$; the ratio of OH^- and H_2O ligands was not determined. The value of $\Delta\varepsilon^{296nm}$ was taken equal to 10540 $M^{-1}cm^{-1}$, i.e. molar absorption coefficient of *trans*-$[Pt^{IV}(Py)_2(N_3)(OH)_2(OH/H_2O)]^{0/+}$ and *trans*-$[Pt^{II}(Py)_2(OH/H_2O)_2]$ were estimated as 10540 $M^{-1}cm^{-1}$ and zero.

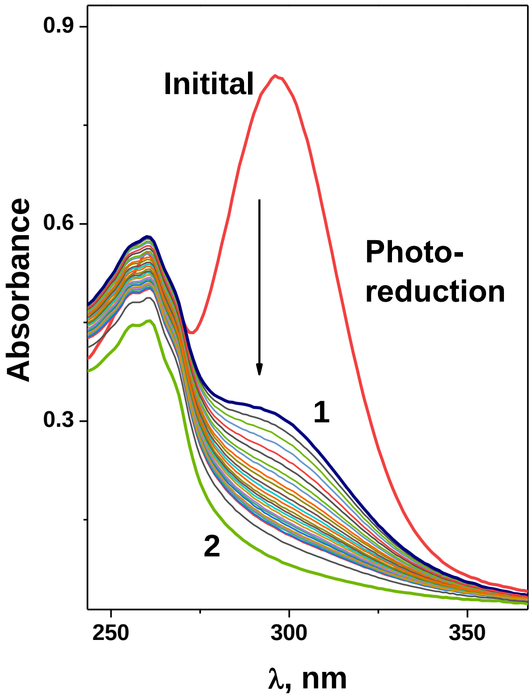

Figure S4. Changes in the UV spectrum of complex **1** (4.3×10^{-5} M, 1 cm cell, air-saturated aqueous solution) in the course of stationary photolysis (308 nm). Second stage (photoreduction). Curves 1 and 2 correspond to 212 and 1412 c of irradiation.

The estimated value of the *trans*-$[Pt^{IV}(Py)_2(N_3)(OH)_2(OH/H_2O)]^{0/+}$ quantum yield was 0.012, i.e. an order of magnitude lower that the quantum yield of the initial complex **1** photoaquation.

S4. Laser flash photolysis of Complex 1

Molar absorption coefficient of Pt(III) intermediate formed by complex **1** photoreduction was estimated using the method described in works [S7, S8]. Briefly, the initial transient absorption was plotted vs. the incident laser pulse energy (Fig. S5). The obtained dependence is linear at low energies with a trend to saturation at higher energies. This type of dependence is typical for a one-photon process. Following the work [S7], we have fitted the experimental curve by function (S2).

$$\Delta D_0 = a(1 - e^{-bE}) \qquad \text{(S2)}$$

E is laser pulse energy, *a*, *b* are parameters of fitting.

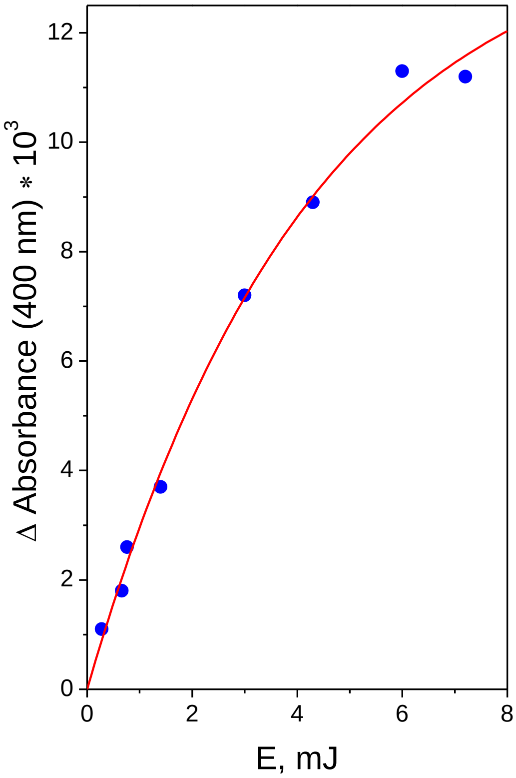

Figure S5. Laser flash photolysis (266 nm) of complex **1** in aqueous solutions (2.4×10^{-5} M, 1 cm cell, air-saturated solutions). Dependence of initial intermediate absorption at 400 nm vs. laser pulse energy. Experimental points and their fit by function (S2) with parameters $a = 14 \pm 1$; $b = (0.23 \pm 0.03)$ mJ^{-1}.

Saturation of the dependence (Fig. S5) could be explained by two factors. First, the intermediate photolysis product could absorbs at the wavelength of excitation (266 nm), and the characteristic time of its formation could be small in comparison with the laser pulse duration (5 ns). In this case, the new product should compete for the light quanta with the initial complex **1**, which should result in saturation of the dependence of intermediate absorption vs. laser pulse energy [S8]. However, in our case the intermediate does not absorb significantly in the region of wavelengths shorter that 300 nm (see Fig. 3b of the main text), and the corresponding explanation of saturation could be ruled out.

Another explanation of saturation is the consumption of all the incident light quanta by complex **1**. Assume that all the irradiated complexes are converted to products; the further increase in light quanta flux would not result in the intermediate absorption increase. Therefore, fitting parameter *a* in Eq. S2 allowed us to estimate molar absorption coefficient of intermediate ($\varepsilon_{\mathrm{int}}$)

$$a = \varepsilon_{int} c_0 l \tag{S3}$$

where c_0 is the concentration of the initial complex **1**, *l* is the optical path length (1 cm). For the maximum of intermediate absorption (400 nm) we obtain $\varepsilon_{\mathrm{int}}^{400\ \mathrm{nm}} = 4200 \pm 1100\ \mathrm{M}^{-1}\mathrm{cm}^{-1}$.

References

[S1] E. Sosnin, T. Oppenlander and V. Tarasenko, *J. Photochem. Photobiol. C: Photochem. Rev.*, 2006, **7**, 145.

[S2] K. C. Kurien, *J. Chem. Soc. B*, 1971, 2081.

[S3] I. P. Pozdnyakov, V. F. Plyusnin, V. P. Grivin, D. Yu. Vorobyev, N. M. Bazhin, S. Pages and E. Vauthey, *J. Photochem. Photobiol. A: Chem*., 2006, **181**, 37.

[S4] E. M. Glebov, V. P. Grivin, V. F. Plyusnin, R. G. Fedunov, I. P. Pozdnyakov, V. V. Yanshole and D. B. Vasilchenko, *J. Photochem. Photobiol. A: Chem*., 2021, **418**, 113440.

[S5] N. J. Farrer, J. A. Woods, L. Salassa, Y. Zhao, K. S. Robinson, G. Clarkson, F. S. Mackay and P. J. Sadler, *Angew. Chem. Int. Ed.*, 2010, **49**, 8905.

[S6] R. R. Vernooij, T. Joshi, M. D. Horbury, B. Graham, E. I. Izgorodina, V. G. Stavros, P. J. Sadler, L. Spiccia and B. R. Wood, *Chem. Eur. J.*, 2018, **24**, 5790.

[S7] U. Lachish, A. Shafferman and G. Stein, *J. Chem. Phys.*, 1976, **64**, 4205.

[S8] S. G Matveeva, I. P. Pozdnyakov, V. P. Grivin, V. F. Plyusnin, A. S. Mereshchenko, A. A. Melnikov, S. V. Chekalin and E. M. Glebov, *J. Photochem. Photobiol. A: Chem*., 2016, **325**, 13.